Worldwide Reactor Neutrino Propagation to Underground Labs: Matter Effects and Flux Predictions

Keyu Han
Tsinghua University

Reactor Prediction Inputs and Data Sources

The reactor-antineutrino prediction combines several public data sources:

- **Reactor operating fleet:**
  IAEA PRIS / IAEA-OPEX 2025 / INFN Ferrara reactor databas

- **Future reactor configurations:**
  World Nuclear Association reactor database and Global Nuclear Power Tracker

- **Reactor spectrum and fission inputs:**
SM2023 spectra for 235U, 238U, 239Pu, and 241Pu
default fission fractions and fission energies from Baldoncini et al(2015).
The IBD total cross section is evaluated using the analytical approximation of Strumia and Vissani

- **Oscillation inputs:**
  PDG 2025 neutrino-oscillation parameters

- **Detector targets:**
  underground laboratory coordinates collected from literature

Goal:
predict reactor $\bar{\nu}$ e fluxes and IBD event rates at underground laboratories, with vacuum, 1D Earth, and 3D Earth matter treatments.

From IAEA/OPEX 2025:
- reactor status
- reactor type
- electrical / thermal power
- annual load factor

From INFN Ferrara:
- reactor-site coordinates

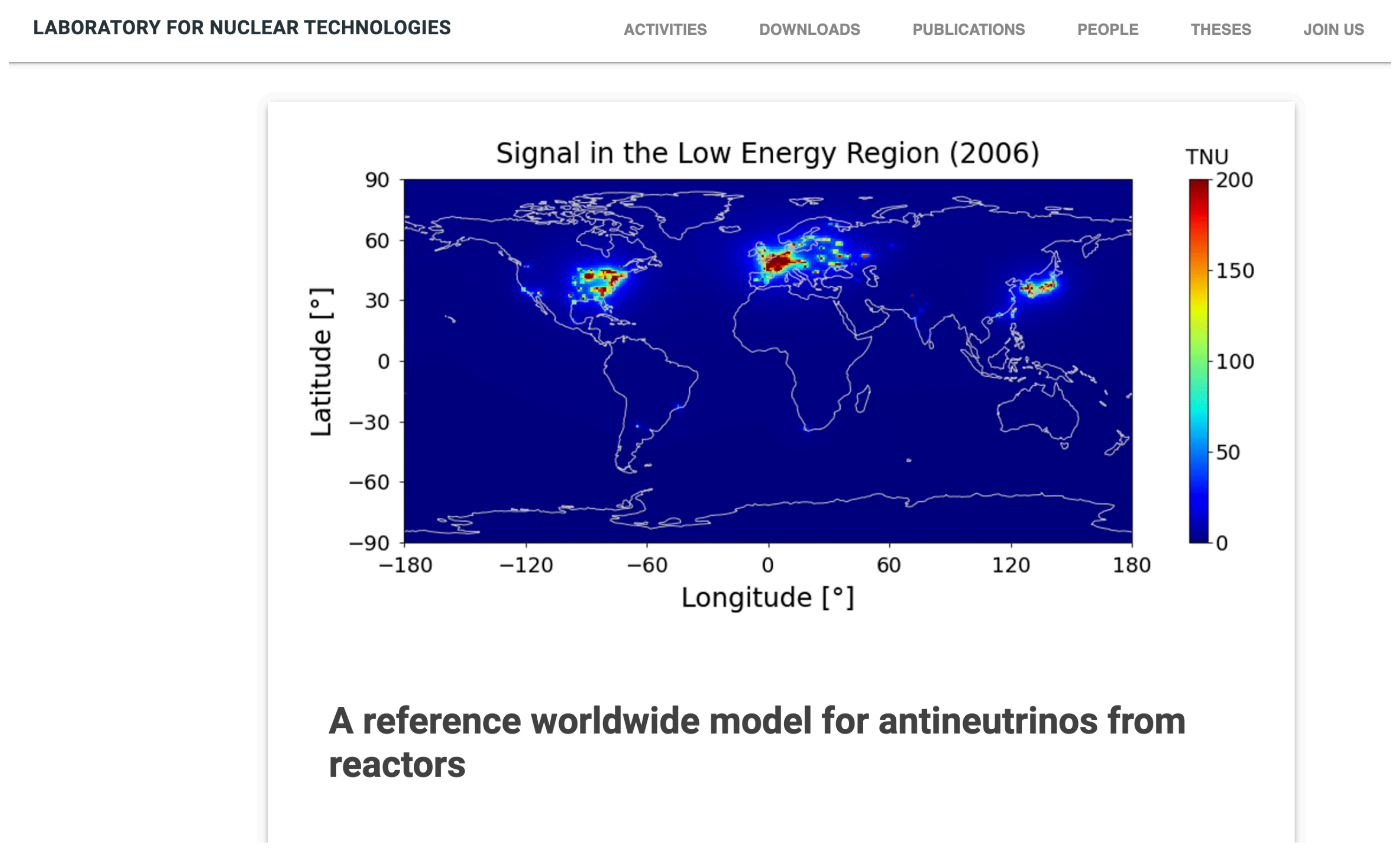

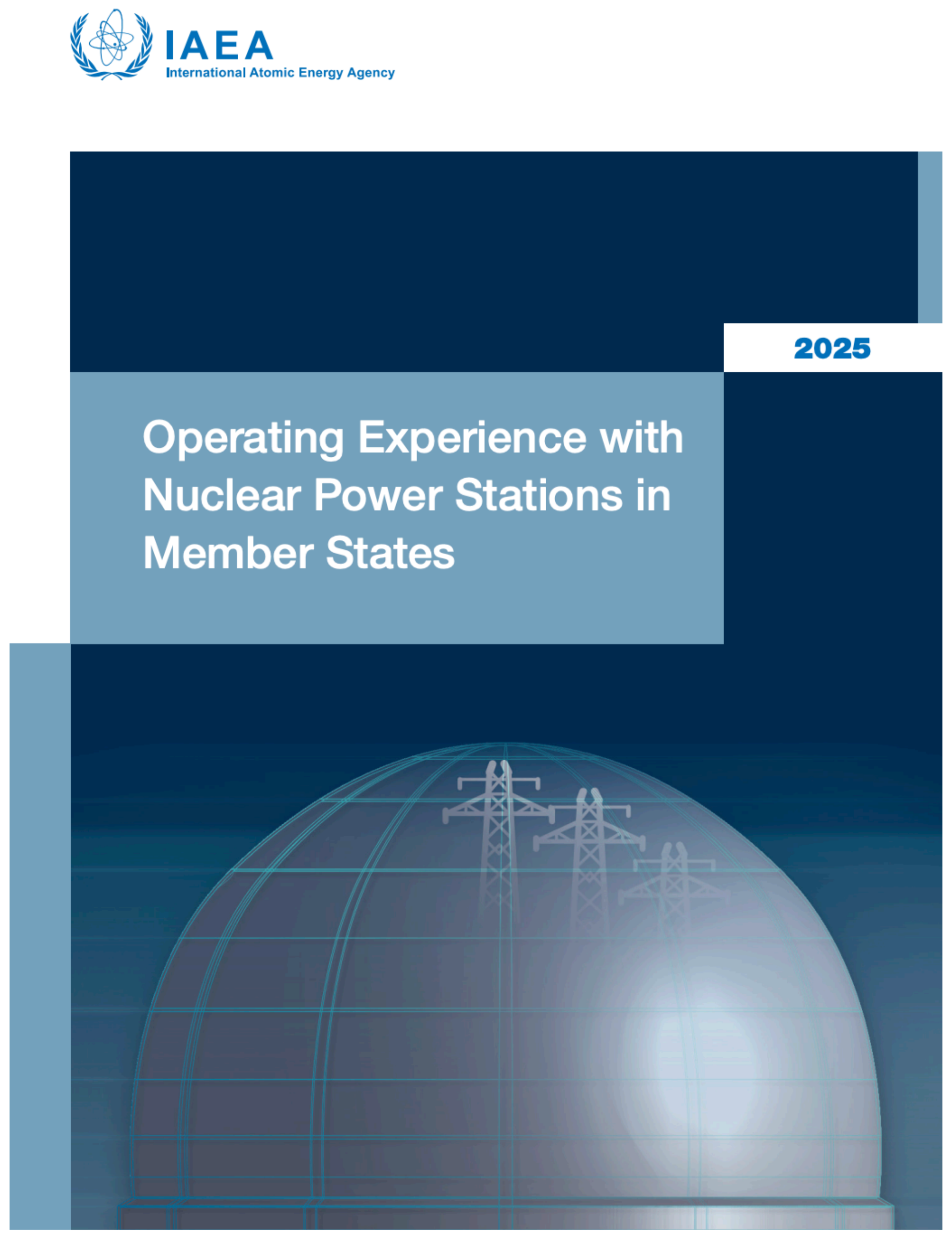

Reactor Prediction Inputs and Data Sources

The reactor-antineutrino prediction combines several public data sources:

- **Reactor operating fleet:**
  IAEA PRIS / IAEA-OPEX 2025 / INFN Ferrara reactor databas

- **Future reactor configurations:**
  World Nuclear Association reactor database and Global Nuclear Power Tracker

- **Reactor spectrum and fission inputs:**
SM2023 spectra for 235U, 238U, 239Pu, and 241Pu
default fission fractions and fission energies from Baldoncini et al(2015).
The IBD total cross section is evaluated using the analytical approximation of Strumia and Vissani

- **Oscillation inputs:**
  PDG 2025 neutrino-oscillation parameters

- **Detector targets:**
  underground laboratory coordinates collected from literature

Goal:
predict reactor $\bar{\nu}$ e fluxes and IBD event rates at underground laboratories, with vacuum, 1D Earth, and 3D Earth matter treatments.

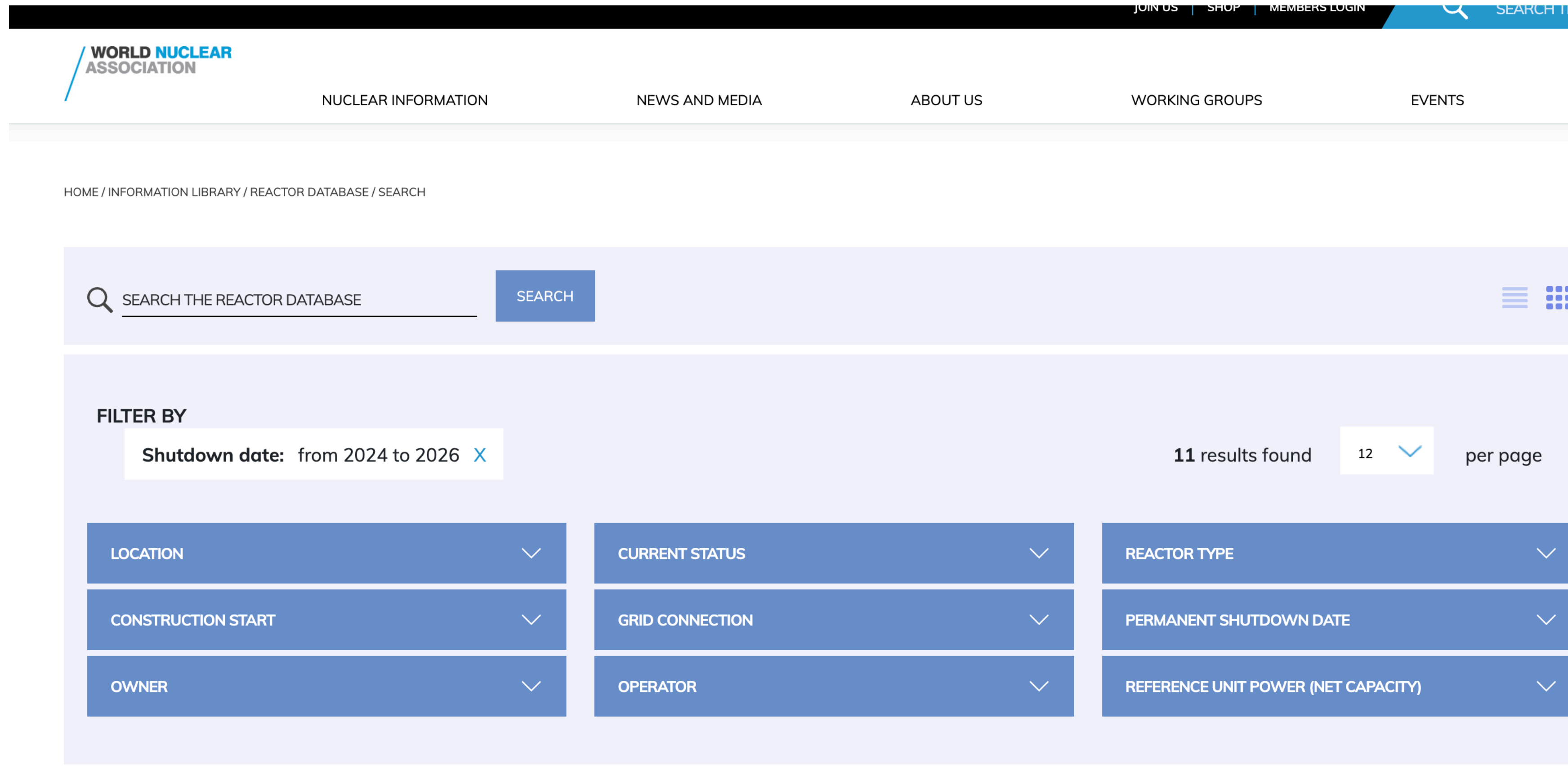

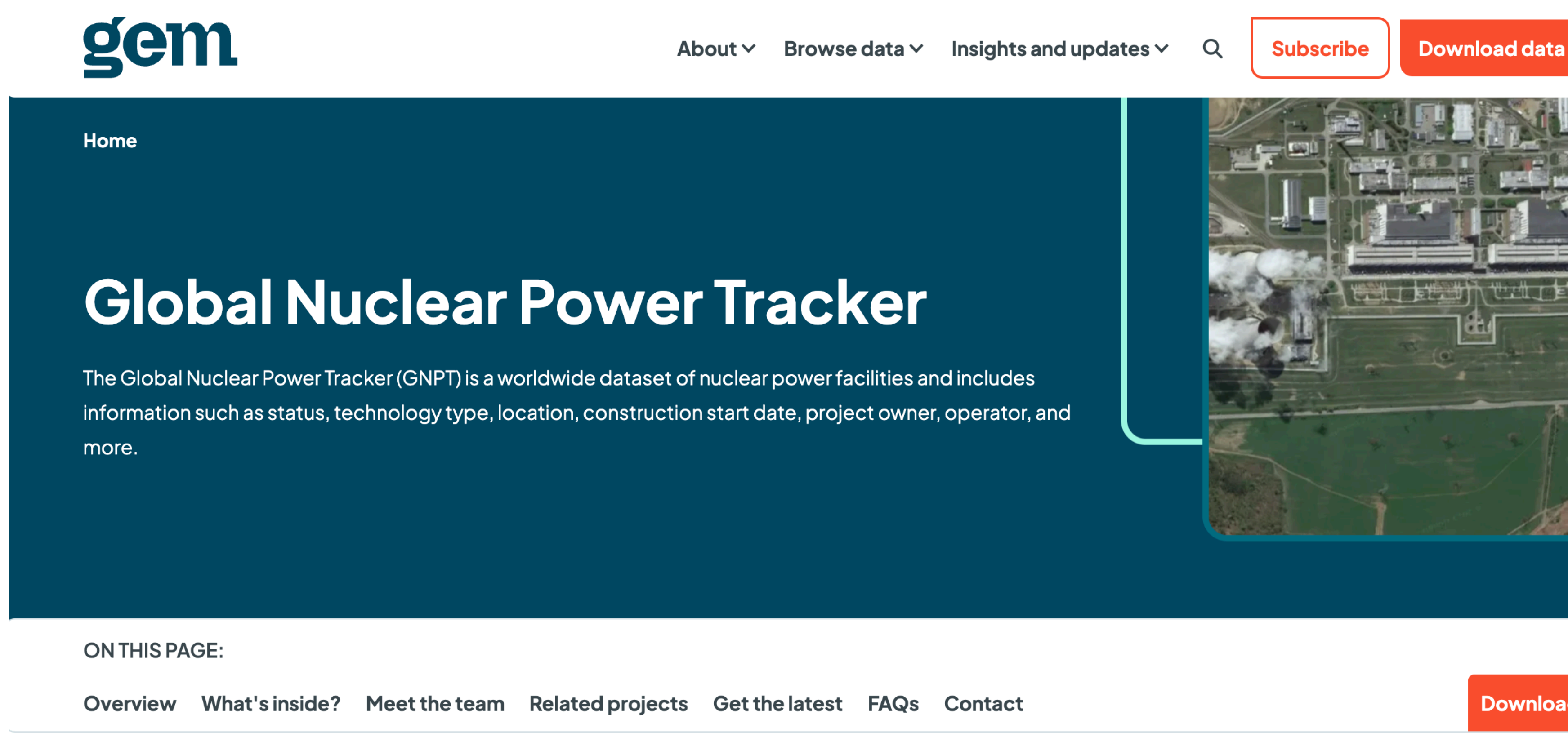

From WNA/GNPT
- future reactor status
- construction progress
- grid connection schedule
- permanent shutdown dates

Reactor Prediction Inputs and Data Sources

The reactor-antineutrino prediction combines several public data sources:

- **Reactor operating fleet:**
  IAEA PRIS / IAEA-OPEX 2025 / INFN Ferrara reactor databas

- **Future reactor configurations:**
  World Nuclear Association reactor database and Global Nuclear Power Tracker

- **Reactor spectrum and fission inputs:**
  SM2023 spectra for 235U, 238U, 239Pu, and 241Pu
  default fission fractions and fission energies from Baldoncini et al(2015).
  The IBD total cross section is evaluated using the analytical approximation of Strumia and Vissani

- **Oscillation inputs:**
  PDG 2025 neutrino-oscillation parameters

- **Detector targets:**
  underground laboratory coordinates collected from literature

Goal:
predict reactor $\bar{\nu}$ e fluxes and IBD event rates at underground laboratories,
with vacuum, 1D Earth, and 3D Earth matter treatments.

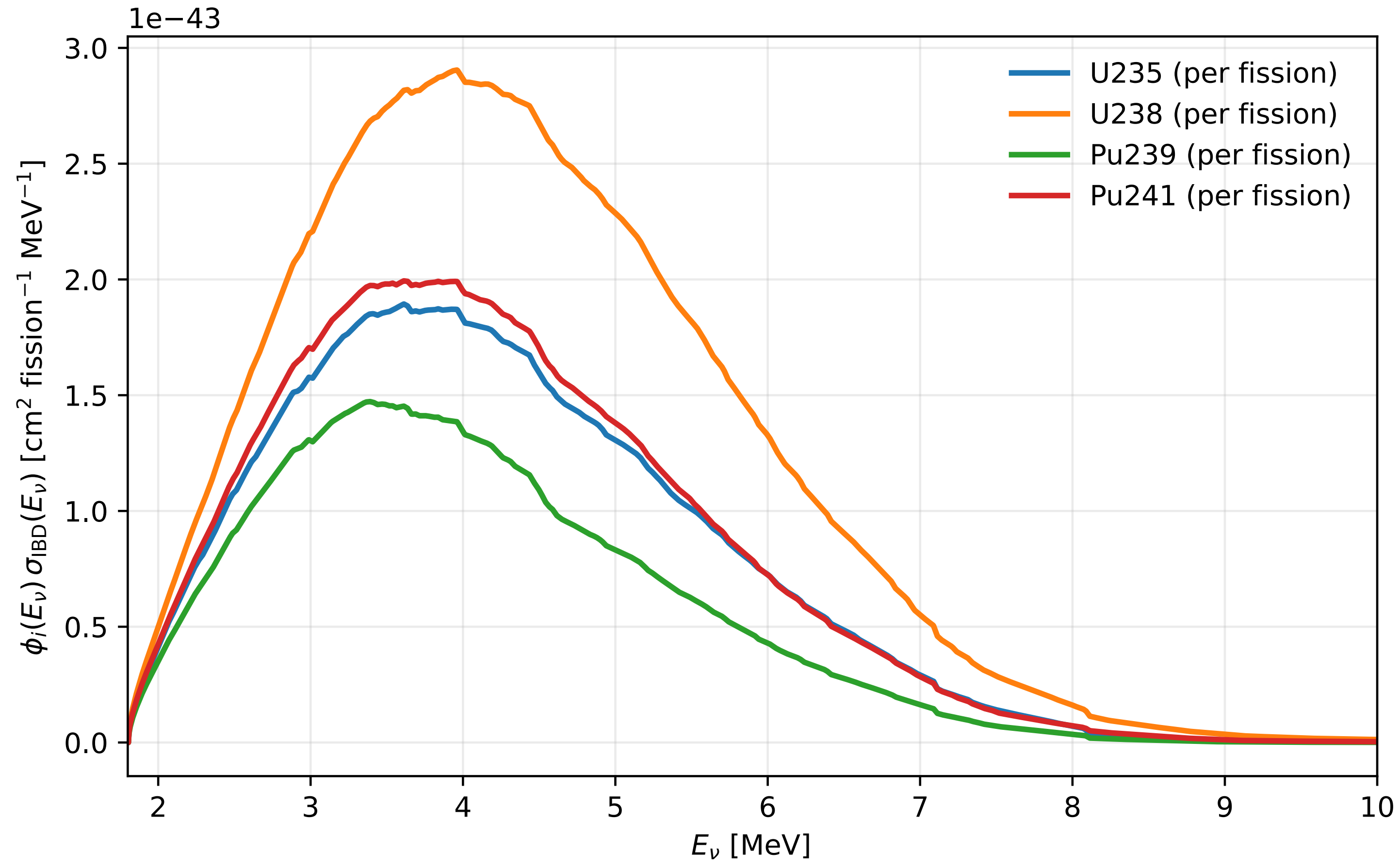

Reactor class	f_{235}	f_{238}	f_{239}	f_{241}
PWR	0.606	0.074	0.274	0.046
BWR	0.488	0.087	0.359	0.067
LWGR	0.580	0.074	0.292	0.054
GCR	0.544	0.075	0.318	0.063
PHWR	0.520	0.050	0.420	0.010
MOX	0.000	0.083	0.708	0.209

Fissile isotope	Q_i (MeV)
^{235}U	202.36 ± 0.26
^{238}U	205.99 ± 0.52
^{239}Pu	211.12 ± 0.34
^{241}Pu	214.26 ± 0.33

Reactor Prediction Inputs and Data Sources

The reactor-antineutrino prediction combines several public data sources:

- **Reactor operating fleet:**
  IAEA PRIS / IAEA-OPEX 2025 / INFN Ferrara reactor databas

- **Future reactor configurations:**
  World Nuclear Association reactor database and Global Nuclear Power Tracker

- **Reactor spectrum:**
  SM2023 summation-model spectra for 235U, 238U, 239Pu and 241Pu

- **Oscillation inputs:**
  PDG 2025 neutrino-oscillation parameters

- **Detector targets:**
  underground laboratory coordinates collected from literature

Goal:
predict reactor $\bar{\nu}$ e fluxes and IBD event rates at underground laboratories, with vacuum, 1D Earth, and 3D Earth matter treatments.

	Ref. [193] w/o SK-ATM & IC24		Ref. [193] w SK-ATM & IC24		Ref. [194] w SK-ATM & IC24	
NO	$\Delta\chi^2 = 0.6$		Best Fit Ordering		Best Fit Ordering	
Param	bfp $\pm 1\sigma$	3σ range	bfp $\pm 1\sigma$	3σ range	bfp $\pm 1\sigma$	3σ range
$\frac{\sin^2\theta_{12}}{10^{-1}}$	$3.07^{+0.12}_{-0.11}$	$2.75 \to 3.45$	$3.08^{+0.12}_{-0.11}$	$2.75 \to 3.45$	$3.03^{+0.14}_{-0.12}$	$2.64 \to 3.45$
$\theta_{12}/°$	$33.68^{+0.73}_{-0.70}$	$31.63 \to 35.95$	$33.68^{+0.73}_{-0.70}$	$31.63 \to 35.95$	$33.40^{+0.87}_{-0.75}$	$30.92 \to 35.97$
$\frac{\sin^2\theta_{23}}{10^{-1}}$	$5.61^{+0.12}_{-0.15}$	$4.30 \to 5.96$	$4.70^{+0.17}_{-0.13}$	$4.35 \to 5.85$	$4.73^{+0.23}_{-0.13}$	$4.37 \to 5.81$
$\theta_{23}/°$	$48.5^{+0.7}_{-0.9}$	$41.0 \to 50.4$	$43.3^{+1.0}_{-0.9}$	$41.3 \to 49.9$	$43.4^{+1.3}_{-0.8}$	$41.4 \to 49.7$
$\frac{\sin^2\theta_{13}}{10^{-2}}$	$2.195^{+0.054}_{-0.058}$	$2.023 \to 2.376$	$2.215^{+0.056}_{-0.058}$	$2.030 \to 2.388$	$2.23^{+0.04}_{-0.06}$	$2.06 \to 2.38$
$\theta_{13}/°$	$8.52^{+0.11}_{-0.11}$	$8.18 \to 8.87$	$8.56^{+0.11}_{-0.11}$	$8.19 \to 8.89$	$8.59^{+0.08}_{-0.12}$	$8.25 \to 8.87$
$\delta_{CP}/°$	177^{+19}_{-20}	$96 \to 422$	212^{+26}_{-41}	$124 \to 364$	216^{+31}_{-23}	$131 \to 365$
$\frac{\Delta m^2_{21}}{10^{-5}\ \mathrm{eV}^2}$	$7.49^{+0.19}_{-0.20}$	$6.92 \to 8.05$	$7.49^{+0.19}_{-0.20}$	$6.92 \to 8.05$	$7.37^{+0.15}_{-0.16}$	$6.93 \to 7.93$
$\frac{\Delta m^2_{32}}{10^{-3}\ \mathrm{eV}^2}$	$2.459^{+0.025}_{-0.023}$	$2.388 \to 2.531$	$2.438^{+0.021}_{-0.019}$	$2.376 \to 2.503$	$2.458^{+0.020}_{-0.020}$	$2.396 \to 2.521$
IO	Best Fit Ordering		$\Delta\chi^2 = 6.1$		$\Delta\chi^2 = 5.0$	
$\frac{\sin^2\theta_{12}}{10^{-1}}$	$3.08^{+0.12}_{-0.11}$	$2.75 \to 3.45$	$3.08^{+0.12}_{-0.11}$	$2.75 \to 3.45$	$3.03^{+0.14}_{-0.12}$	$2.64 \to 3.45$
$\theta_{12}/°$	$33.68^{+0.73}_{-0.70}$	$31.63 \to 35.95$	$33.68^{+0.73}_{-0.70}$	$31.63 \to 35.95$	$33.40^{+0.87}_{-0.75}$	$30.92 \to 35.97$
$\frac{\sin^2\theta_{23}}{10^{-1}}$	$5.62^{+0.12}_{-0.15}$	$4.37 \to 5.97$	$5.50^{+0.12}_{-0.15}$	$4.40 \to 5.84$	$5.45^{+0.15}_{-0.17}$	$4.43 \to 5.83$
$\theta_{23}/°$	$48.6^{+0.7}_{-0.9}$	$41.4 \to 50.6$	$47.9^{+0.7}_{-0.9}$	$41.5 \to 49.8$	$47.6^{+0.9}_{-1.0}$	$41.7 \to 50.0$
$\frac{\sin^2\theta_{13}}{10^{-2}}$	$2.224^{+0.056}_{-0.057}$	$2.053 \to 2.397$	$2.221^{+0.056}_{-0.056}$	$2.060 \to 2.409$	$2.23^{+0.07}_{-0.04}$	$2.08 \to 2.41$
$\theta_{13}/°$	$8.58^{+0.11}_{-0.11}$	$8.24 \to 8.91$	$8.59^{+0.11}_{-0.11}$	$8.25 \to 8.93$	$8.59^{+0.13}_{-0.08}$	$8.29 \to 8.93$
$\delta_{CP}/°$	285^{+25}_{-28}	$201 \to 348$	274^{+22}_{-25}	$201 \to 335$	274^{+25}_{-27}	$193 \to 329$
$\frac{\Delta m^2_{21}}{10^{-5}\ \mathrm{eV}^2}$	$7.49^{+0.19}_{-0.19}$	$6.92 \to 8.05$	$7.49^{+0.19}_{-0.19}$	$6.92 \to 8.05$	$7.37^{+0.15}_{-0.16}$	$6.93 \to 7.93$
$\frac{\Delta m^2_{32}}{10^{-3}\ \mathrm{eV}^2}$	$-2.510^{+0.024}_{-0.025}$	$-2.584 \to -2.438$	$-2.484^{+0.020}_{-0.020}$	$-2.547 \to -2.421$	$-2.502^{+0.021}_{-0.020}$	$-2.564 \to -2.440$

Lab	Latitude	Longitude	Country
ANDES [26]	−30.25	−69.883	Argentina
Baksan [27]	43.28	42.69	Russia
Boulby [28]	54.553	−0.825	UK
CallioLab [29]	63.659	26.042	Finland
CJPL	28.2	101.7	China
JUNO [30]	22.118	112.518	China
Kamioka [31]	36.426	137.310	Japan
LNGS [32]	42.450	13.567	Italy
LSC [33]	42.775	−0.529	Spain
LSM [34]	45.200	6.670	France
SNO [35]	46.475	−81.201	Canada
SUPL [26]	−37.050	142.767	Australia
SURF [36]	44.352	−103.752	USA
Yemilab [37]	37.189	128.659	South Korea

Earth Density Models for Matter Effects

1D reference model:

- - PREM radial density profile
- - spherically symmetric
- - density depends only on depth
- - used as the baseline Earth model

Hybrid 3D Earth model:

- - LITHO1.0: 0–320 km
- crust and uppermost mantle

- - SAW642AN: 320–2880 km
- 3D mantle density structure

- - PREM: 2880–6371 km
- deep Earth and core region

- Electron fraction prescription:
- - water / ice: $Y_e = 0.555$
- - crust, sediments, lithospheric plates: $Y_e = 0.50$
- - mantle: $Y_e = 0.50$
- - core: $Y_e = 0.467$

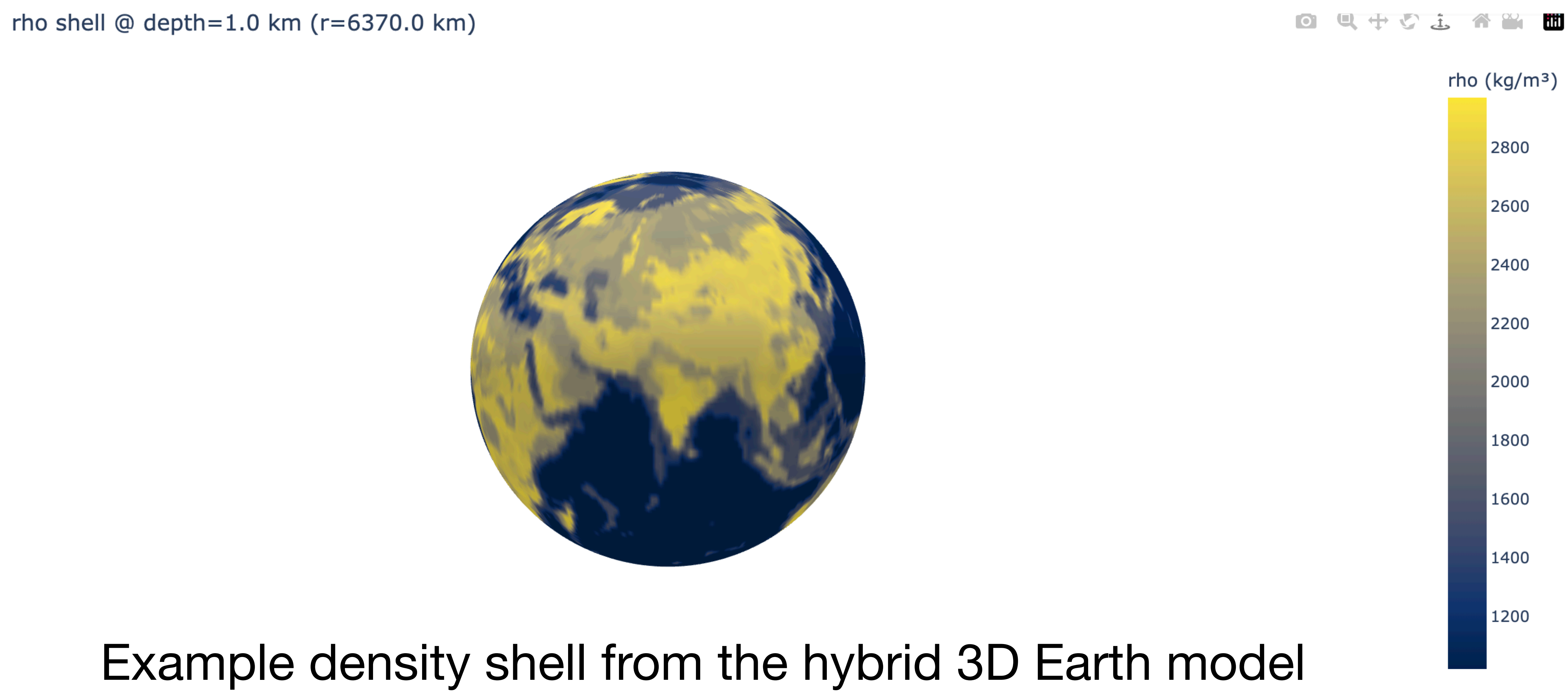

Example density shell from the hybrid 3D Earth model

Computation Method for Earth-Matter Effects

CERN-TH-2016-256

Scanning the Earth with solar neutrinos and DUNE

A. N. Ioannisian[1,2], A.Yu. Smirnov[3,4], D. Wyler[5]
[1] *Yerevan Physics Institute, Alikhanian Br. 2, 375036 Yerevan, Armenia*
[2] *Institute for Theoretical Physics and Modeling, 375036 Yerevan, Armenia*
[3] *Max-Planck Institute for Nuclear Physics, Saupfercheckweg 1, D-69117 Heidelberg, Germany*
[4] *ICTP, Strada Costiera 11, 34014 Trieste, Italy*
[5] *Institut für Theoretische Physik, Universität Zürich, Winterthurerstrasse 190, CH-8057 Zürich, Switzerland*

1^{st}-order rotation approximation:

$$S(x_N = L, 0) = \prod_k e^{-iH_k \Delta x} = \prod_k U_k^m D_k U_k^{m\dagger}$$

$$U_{k,k-1} = U_k^\dagger \, U_{k-1} \approx I - i\lambda_{12}\Delta\theta_{12}:$$

vs

Strang splitting form

$$|\psi_{n+1}\rangle \;=\; e^{-iH_{\mathrm{vac}}\Delta x_n/2}\left[I + \left(e^{-iV_n\Delta x_n} - 1\right) P_e\right] e^{-iH_{\mathrm{vac}}\Delta x_n/2}\,|\psi_n\rangle\,.$$

- analytical first-order treatment of layer-to-layer matter mixing
- used as a cross-check of the MSW solver
- the difference defines the solver-dependence diagnostic Δ_M

- unitary structure is preserved
- matter step is an exact rank-one update
- used for the main 1D/3D Earth predictions

Predictions for CJPL

For CJPL, the MSW prediction gives

$\Phi \simeq 7.48^{+0.19}_{-0.21} \times 10^4 cm^{-2} s^{-1}$

and

$R_{IBD} \simeq 24.30^{+0.84}_{-0.84}$ TNU .

Compared with the vacuum prediction, this corresponds to a small but non-negligible sub-percent enhancement:
about 0.3% in flux and 0.7% in IBD rate.

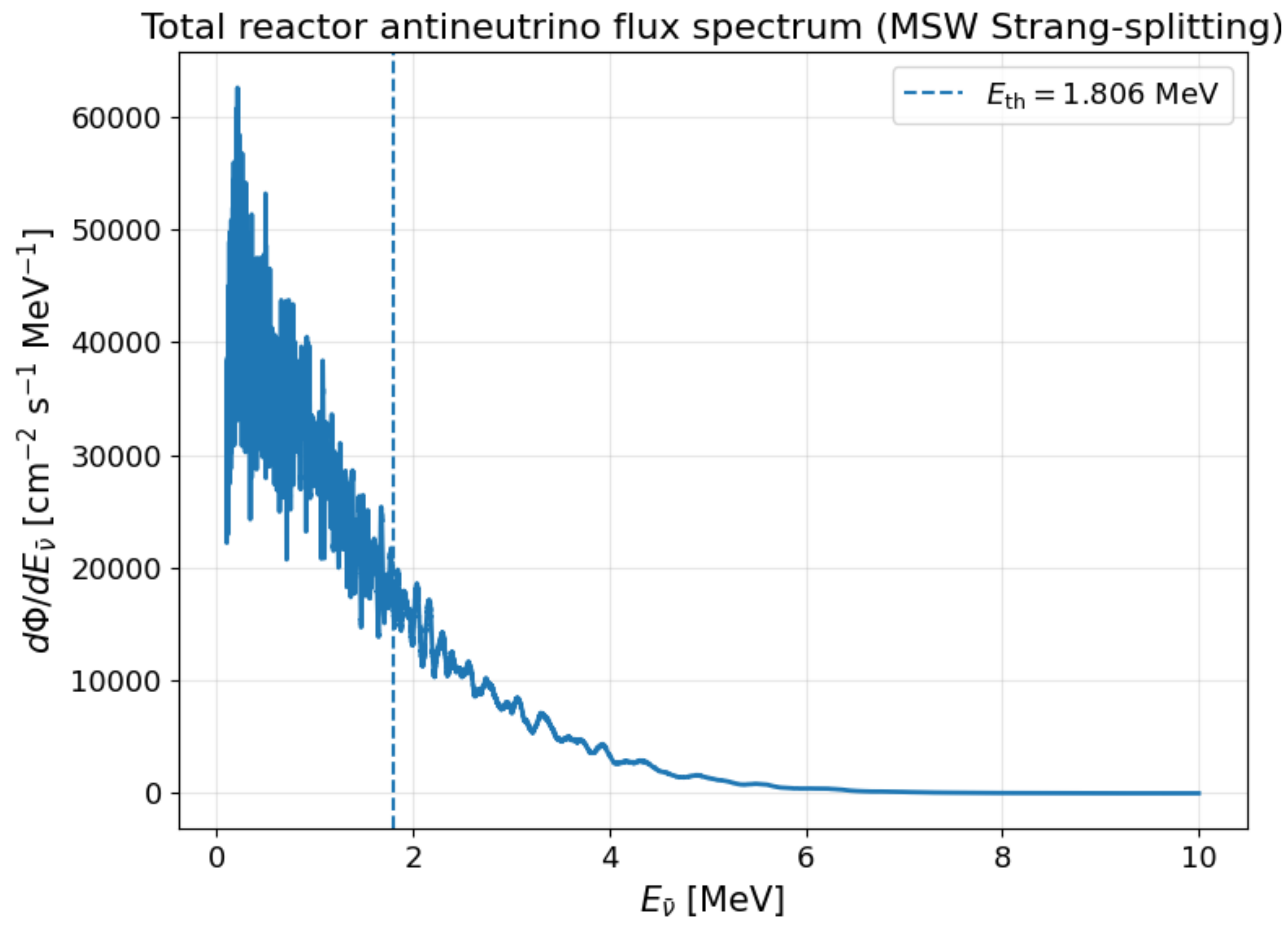

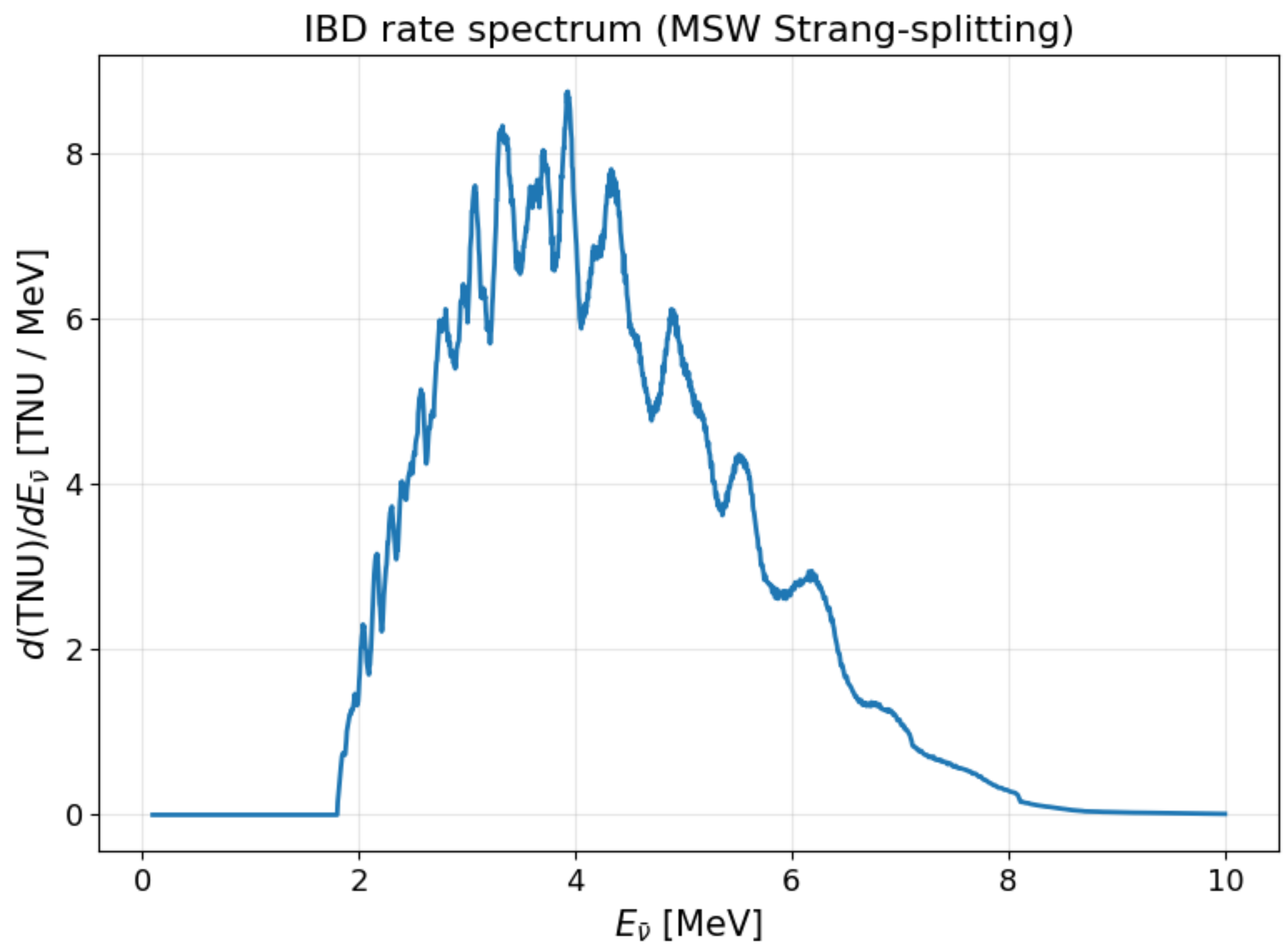

Predictions for Underground Labs

The tables summarize the predicted integrated reactor $\bar{\nu}$ e flux Φ and IBD event rate in TNU for multiple underground laboratories in 2026 and 2030.

For each site, we compare:

- vacuum oscillation prediction
- MSW prediction with the hybrid 3D Earth model
- diagnostic systematic shifts:

  Δ_M: solver dependence

  $\Delta_\oplus$: Earth-model dependence

  $\Delta_{N/I}$: mass-ordering dependence

Main observations:

- Reactor backgrounds are strongly site-dependent.
- JUNO and Yemilab receive the largest reactor $\bar{\nu}_e$ backgrounds.
- CJPL, ANDES, and SUPL remain comparatively clean sites.
- From 2026 to 2030, most sites show moderate changes, while CJPL and Kamioka increase more visibly.
- The MSW correction is small but reaches the sub-percent level.
- Among the diagnostic systematics, the Earth-model dependence $\Delta_\oplus$ is the dominant one.

Table 7.2: Predicted integrated reactor $\bar{\nu}_e$ flux Φ and IBD event rate for underground laboratories in 2026. The MSW columns adopt the three-flavor matter-enhanced neutrino-oscillation formalism, incorporating a three-dimensional Earth-density model and employing the Strang-splitting method as the baseline computational approach. $\Phi\,[\mathrm{cm}^{-2}\,\mathrm{s}^{-1}]$ is integrated over $E_\nu \in [0.1, 10]$ MeV. The definitions for systematic errors $\Delta_\mathcal{M}$, $\Delta_\oplus$, and $\Delta_{\mathrm{N/I}}$ are given in the text.

	Vacuum		MSW		|Syst.|[%]		
Site	Φ $[\times 10^4]$	TNU	Φ $[\times 10^4]$	TNU	$\Delta_\mathcal{M}$	$\Delta_\oplus$	$\Delta_{\mathrm{N/I}}$
ANDES	$1.46^{+0.04}_{-0.04}$	$4.64^{+0.16}_{-0.16}$	$1.46^{+0.04}_{-0.04}$	$4.67^{+0.12}_{-0.12}$	0.01	0.19	0.02
Baksan	$13.64^{+0.33}_{-0.41}$	$43.97^{+1.55}_{-1.53}$	$13.66^{+0.34}_{-0.40}$	$44.23^{+1.57}_{-1.51}$	0.00	0.32	0.02
Boulby	$248.01^{+8.20}_{-8.11}$	$1074.93^{+40.65}_{-40.02}$	$248.36^{+8.29}_{-7.96}$	$1075.99^{+40.24}_{-40.50}$	0.00	0.05	0.02
CallioLab	$22.20^{+0.66}_{-0.54}$	$72.10^{+2.50}_{-2.51}$	$22.25^{+0.66}_{-0.53}$	$72.55^{+2.54}_{-2.49}$	0.00	0.35	0.01
CJPL	$7.46^{+0.19}_{-0.21}$	$24.14^{+0.84}_{-0.83}$	$7.48^{+0.19}_{-0.21}$	$24.30^{+0.84}_{-0.84}$	0.02	0.22	0.03
JUNO	$669.58^{+19.75}_{-20.91}$	$1367.09^{+75.55}_{-69.99}$	$671.51^{+19.84}_{-20.79}$	$1379.98^{+78.21}_{-71.11}$	0.02	0.53	0.03
Kamioka	$58.37^{+1.62}_{-1.56}$	$199.13^{+6.86}_{-6.84}$	$58.48^{+1.63}_{-1.54}$	$199.90^{+6.90}_{-6.82}$	0.01	0.22	0.02
LNGS	$21.46^{+0.53}_{-0.61}$	$69.37^{+2.40}_{-2.39}$	$21.48^{+0.55}_{-0.59}$	$69.77^{+2.43}_{-2.38}$	0.01	0.34	0.02
LSC	$66.81^{+1.62}_{-1.98}$	$218.71^{+7.57}_{-7.44}$	$66.94^{+1.65}_{-1.95}$	$219.75^{+7.63}_{-7.42}$	0.01	0.31	0.02
LSM	$137.49^{+3.45}_{-3.90}$	$474.23^{+16.09}_{-16.51}$	$137.79^{+3.48}_{-3.85}$	$476.88^{+16.30}_{-16.44}$	0.01	0.35	0.02
SNO	$55.93^{+1.61}_{-1.37}$	$175.34^{+6.21}_{-6.07}$	$56.04^{+1.63}_{-1.35}$	$176.37^{+6.30}_{-6.03}$	0.01	0.36	0.02
SUPL	$0.78^{+0.03}_{-0.01}$	$2.53^{+0.09}_{-0.09}$	$0.79^{+0.02}_{-0.02}$	$2.55^{+0.09}_{-0.09}$	0.01	0.02	0.00
SURF	$9.21^{+0.25}_{-0.24}$	$29.69^{+1.02}_{-1.02}$	$9.24^{+0.25}_{-0.24}$	$29.90^{+1.04}_{-1.02}$	0.03	0.25	0.03
Yemilab	$432.53^{+11.10}_{-13.13}$	$908.08^{+43.71}_{-41.78}$	$433.45^{+11.34}_{-12.85}$	$917.77^{+45.20}_{-40.68}$	0.01	0.51	0.03

Table 7.3: Predicted integrated reactor $\bar{\nu}_e$ flux Φ and IBD event rate for underground laboratories in 2030. The MSW columns adopt the three-flavor matter-enhanced neutrino-oscillation formalism, incorporating a three-dimensional Earth-density model and employing the Strang-splitting method as the baseline computational approach. $\Phi\,[\mathrm{cm}^{-2}\,\mathrm{s}^{-1}]$ is integrated over $E_\nu \in [0.1, 10]$ MeV. $\Phi\,[\mathrm{cm}^{-2}\,\mathrm{s}^{-1}]$ is integrated over $E_\nu \in [0.1, 10]$ MeV. The definitions for systematic errors $\Delta_\mathcal{M}$, $\Delta_\oplus$, and $\Delta_{\mathrm{N/I}}$ are given in the text.

	Vacuum		MSW		|Syst.|[%]		
Site	Φ $[\times 10^4]$	TNU	Φ $[\times 10^4]$	TNU	$\Delta_\mathcal{M}$	$\Delta_\oplus$	$\Delta_{\mathrm{N/I}}$
ANDES	$1.49^{+0.04}_{-0.04}$	$4.75^{+0.17}_{-0.16}$	$1.50^{+0.04}_{-0.04}$	$4.78^{+0.17}_{-0.17}$	0.01	0.18	0.02
Baksan	$14.42^{+0.35}_{-0.42}$	$46.50^{+1.63}_{-1.61}$	$14.44^{+0.36}_{-0.41}$	$46.78^{+1.66}_{-1.60}$	0.00	0.31	0.01
Boulby	$251.64^{+8.20}_{-8.25}$	$1086.67^{+41.02}_{-40.36}$	$251.99^{+8.34}_{-8.09}$	$1087.78^{+40.71}_{-40.89}$	0.00	0.05	0.02
CallioLab	$23.54^{+0.68}_{-0.58}$	$76.45^{+2.65}_{-2.66}$	$23.60^{+0.69}_{-0.57}$	$76.93^{+2.69}_{-2.64}$	0.00	0.35	0.00
CJPL	$8.30^{+0.21}_{-0.23}$	$26.83^{+0.92}_{-0.93}$	$8.33^{+0.21}_{-0.24}$	$27.00^{+0.93}_{-0.93}$	0.02	0.21	0.03
JUNO	$676.23^{+19.84}_{-21.14}$	$1388.25^{+76.11}_{-70.53}$	$678.17^{+20.33}_{-20.70}$	$1401.25^{+76.35}_{-70.02}$	0.02	0.52	0.03
Kamioka	$70.65^{+1.92}_{-1.91}$	$242.53^{+8.35}_{-8.34}$	$70.78^{+1.95}_{-1.88}$	$243.49^{+8.39}_{-8.31}$	0.01	0.23	0.02
LNGS	$22.09^{+0.54}_{-0.63}$	$71.40^{+2.47}_{-2.46}$	$22.11^{+0.57}_{-0.61}$	$71.80^{+2.50}_{-2.45}$	0.01	0.34	0.02
LSC	$67.62^{+1.63}_{-2.01}$	$221.29^{+7.65}_{-7.53}$	$67.75^{+1.66}_{-1.97}$	$222.35^{+7.73}_{-7.49}$	0.01	0.31	0.02
LSM	$138.34^{+3.45}_{-3.93}$	$476.94^{+16.18}_{-16.60}$	$138.64^{+3.49}_{-3.88}$	$479.61^{+16.36}_{-16.51}$	0.01	0.35	0.02
SNO	$55.98^{+1.61}_{-1.37}$	$175.51^{+6.23}_{-6.08}$	$56.09^{+1.63}_{-1.35}$	$176.53^{+6.31}_{-6.03}$	0.01	0.36	0.02
SUPL	$0.85^{+0.03}_{-0.02}$	$2.76^{+0.10}_{-0.10}$	$0.86^{+0.02}_{-0.02}$	$2.78^{+0.10}_{-0.10}$	0.00	0.02	0.01
SURF	$9.13^{+0.25}_{-0.24}$	$29.43^{+1.02}_{-1.01}$	$9.16^{+0.24}_{-0.24}$	$29.64^{+1.03}_{-1.01}$	0.03	0.25	0.04
Yemilab	$436.86^{+11.16}_{-13.26}$	$922.07^{+43.97}_{-42.26}$	$437.79^{+11.42}_{-12.94}$	$931.85^{+45.43}_{-41.14}$	0.01	0.51	0.03